Letters

Free-Rotation Wireless Power Transfer System Based on Composite Anti-Misalignment Method for AUVs

Zhengchao Yan, *Member, IEEE*, Min Wu, Chenxu Zhao, Qianyu Hu, Lei Zhu, Lin Qiao, and Laili Wang, *Senior Member, IEEE*

***Abstract*—In the underwater environment, the ocean current will have a great influence on the anti-misalignment performance of the wireless power transfer (WPT) system for the autonomous underwater vehicles (AUVs). In this letter, a free-rotation WPT system with a new magnetic coupler for AUVs is proposed to improve the rotational and axial misalignment tolerance. The magnetic coupler has two decoupled transmitters and one segmented arc solenoid receiver with reversely wound adjacent receiver coils. The mutual inductances between the receiver and the two transmitters can compensate each other. Moreover, cooperated with the phase control between the two transmitters, the system can achieve more stable output power under the rotational and axial misalignment. A free-rotation WPT prototype was set up and the experimental results showed that the output power can reach 700 W and the output power fluctuation is below 5% based on the proposed anti-misalignment method.**

***Index Terms*—Anti-misalignment, autonomous underwater vehicle (AUV), free-rotation, wireless power transfer (WPT).**

I. Introduction

WIRELESS power transfer (WPT) is a promising technology that has advantages in diverse scenarios, such as electric vehicles [1], [2], [3], trains [4], and underwater equipment like autonomous underwater vehicles (AUVs) [5], [6]. The magnetically coupled resonant WPT technology is an effective way to solve the energy issue of the AUV to achieve long-term continuous work. The power can be delivered to the battery of the AUV wirelessly without any direct contact, which improves the safety and concealment of the system. In the underwater environment, the ocean current will cause misalignments on the transmitter side and receiver sides, which has a great influence on the power transfer stability of the WPT system for AUVs.

There are three methods to improve the misalignment tolerance of the WPT system. First, the misalignment tolerance can be improved through magnetic coupler design. To improve the rotational misalignment tolerance, a hull-compatible magnetic coupler based on the solenoid coil structure was proposed, which can deliver 45 W of power at 84% efficiency [7], [8]. While the magnetic field of the system is divergent. Thus, a light-weight WPT system was proposed to enhance the rotational misalignment performance and converge the magnetic field [9]. Another WPT system based on three transmitters with different phases was proposed, while the system efficiency and the output power were unstable. The dc–dc efficiency varies from 76.24% to 86.19%, and the output power ranges from 321 to 745 W during the rotational misalignment [10]. Then a WPT system based on a new magnetic coupler with two double-layer receivers was proposed. The dc–dc efficiency is 92.10%–92.26%, and the output power can achieve from 485 to 664 W [11]. Second, the misalignment tolerance can be improved through hybrid compensation topology design. A hybrid WPT system was proposed that took advantage of a combination of series–series (S–S) and LCC–LCC compensation topologies to achieve constant charging power against the large pad misalignment [12]. Finally, the misalignment tolerance can be improved through the system control method [13]. Orekan et al. [14] proposed a maximum power efficiency tracking method with the real-time changing duty cycle of the dc–dc converter to achieve the stable output under the misalignment.

It is limited to improving the antimisalignment tolerance by a single method. Thus, the cooperation strategy of multiple antimisalignment methods should be adopted to solve the large and multidirection misalignment issue. In this letter, a free-rotation WPT system with a new magnetic coupler for AUVs is proposed to improve the rotational misalignment tolerance. The magnetic coupler design and phase control method, which is called the composite anti-misalignment method, are adopted to achieve stable output power under rotational misalignment. A free-rotation WPT system is established to verify the proposed composite anti-misalignment method.

Manuscript received 15 November 2022; revised 4 December 2022 and 29 December 2022; accepted 13 January 2023. Date of publication 19 January 2023; date of current version 14 February 2023. This work was supported in part by the National Natural Science Foundation of China under Grant 52201405, in part by the China Postdoctoral Science Foundation under Grant 2020TQ0237 and Grant 2021M702555, and in part by the Power Electronics Science and Education Development Program of Delta Group. *(Corresponding author: Laili Wang.)*

Zhengchao Yan, Min Wu, Chenxu Zhao, Qianyu Hu, Lei Zhu, and Laili Wang are with the School of Electrical Engineering, Xi'an Jiaotong University, Xi'an 710049, China (e-mail: yanzc1991@gmail.com; wm3117079009@stu.xjtu.edu.cn; zhaochenxu@stu.xjtu.edu.cn; hqy_23@163.com; jasmine@stu.xjtu.edu.cn; llwang@mail.xjtu.edu.cn).

Lin Qiao is with the Power Department, Xi'an Action Power Electric Co., Ltd, Xi'an 710119, China (e-mail: qiaolin0212@163.com).

Color versions of one or more figures in this article are available at https://doi.org/10.1109/TPEL.2023.3238066.

Digital Object Identifier 10.1109/TPEL.2023.3238066

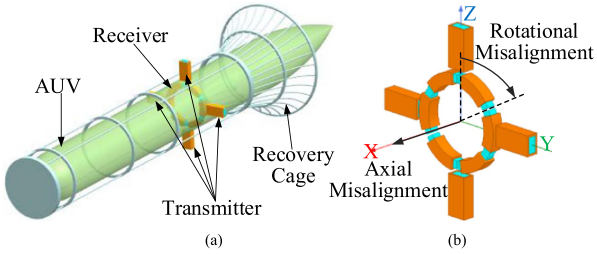

Fig. 1. (a) Overall structure of the free-rotation WPT system for AUV. (b) Definitions of the rotational and axial misalignment.

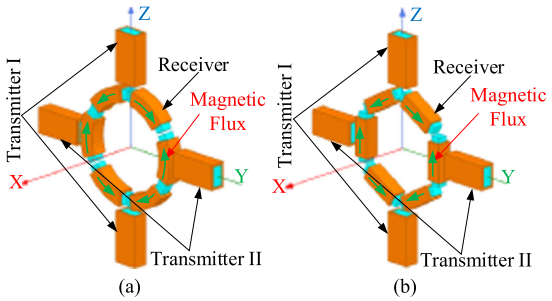

Fig. 2. Magnetic couplers of the free-rotation WPT system for AUV. (a) Ideal. (b) Practical.

II. Coil Design

Fig. 1(a) shows the overall structure of the WPT system based on the proposed magnetic coupler, and Fig 1(b) shows the definitions of the rotational and axial misalignments. The transmitters are fixed to the recovery cage of the seafloor base station for charging the AUVs, and the receiver is embedded into the hull of the AUV. When the AUV lacks of energy, it will be navigated to the base station and enter the recovery cage. Then the rotational and axial misalignments may occur.

Fig. 2(a) shows the proposed ideal magnetic coupler of the free-rotation WPT system. The magnetic coupler has two transmitters and one receiver. The receiver is designed with a toroidal structure, which consists of six segmented arc solenoid coils. The six receiver coils are series connected and adjacently reversely wound. The transmitters I and II are respectively composed of two series-connected solenoid coils to improve the coupling between the transmitter and receiver. The magnetic fields of the two transmitters are perpendicular to each other, so the two transmitters are decoupled. The mutual inductances of the receiver and the two transmitters can compensate each other to resist the variation of the equivalent mutual inductance of the system.

The cubic ferrite is used in the design due to the unavailability of the arc ferrite. Fig. 2(b) shows the proposed magnetic coupler with the cubic ferrite. To get closer to the magnetic coupler with the arc ferrite, the cubic ferrite length is designed identically to the middle arc length of the arc ferrite. Also, the thickness and width of the cubic ferrite are equal to those of the arc ferrite.

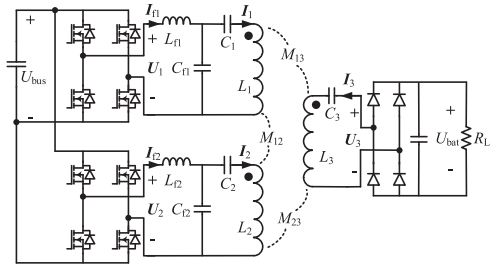

Fig. 3. LCC-S-compensated circuit topology of the proposed WPT system.

III. Circuit Analysis

The circuit topology of the proposed magnetic coupler with two-phase transmitters is shown in Fig. 3, where the LCC-S compensation topology is adopted to maintain the transmitter coil currents constant [15], [16] against the rotational misalignment. L_{f1}, L_{f2} are the compensation inductances, C_{f1}, C_{f2} are the parallel compensation capacitances, C_1, C_2, and C_3 are the series compensation capacitances, L_1, L_2, and L_3 are the self-inductances, U_{bus} and U_{bat} are the input and output dc voltages, U_1 and U_2 are the input ac voltages, I_{f1} and I_{f2} are the input currents, I_1 and I_2 are the transmitter currents, U_3 is the output ac voltage, I_3 is the output current, R_L is the load resistance, $R_E = 8R_L/\pi^2$, is the equivalent resistance before the rectifier, M_{12}, M_{13}, and M_{23} are the mutual inductances among the two transmitters and the receiver.

The resonant condition of the circuit topology is

$$\begin{cases} j\omega_0 L_{f1} + \frac{1}{j\omega_0 C_{f1}} = 0, j\omega_0 L_1 + \frac{1}{j\omega_0 C_1} + \frac{1}{j\omega_0 C_{f1}} = 0 \\ j\omega_0 L_{f2} + \frac{1}{j\omega_0 C_{f2}} = 0, j\omega_0 L_2 + \frac{1}{j\omega_0 C_2} + \frac{1}{j\omega_0 C_{f2}} = 0 \\ j\omega_0 L_3 + \frac{1}{j\omega_0 C_3} = 0 \end{cases} \tag{1}$$

where ω_0 is the resonant angular frequency. If the phase difference between the two inverters is θ, based on the first harmonic approximation, the input voltages $\boldsymbol{U}_1$ and $\boldsymbol{U}_2$ can be expressed as follows:

$$\boldsymbol{U}_1 = \frac{2\sqrt{2}}{\pi} U_{bus} e^{j0^\circ}, \boldsymbol{U}_2 = \frac{2\sqrt{2}}{\pi} U_{bus} e^{j\theta} \tag{2}$$

Based on the Kirchhoff's law and under the resonant condition, the following equation can be obtained.

$$\begin{cases} \boldsymbol{U}_1 = j\omega_0 L_{f1} \boldsymbol{I}_{f1} + \frac{1}{j\omega_0 C_{f1}} (\boldsymbol{I}_{f1} - \boldsymbol{I}_1) \\ \boldsymbol{U}_2 = j\omega_0 L_{f2} \boldsymbol{I}_{f2} + \frac{1}{j\omega_0 C_{f2}} (\boldsymbol{I}_{f2} - \boldsymbol{I}_2) \\ \boldsymbol{U}_3 = j\omega_0 M_{13} \boldsymbol{I}_1 + j\omega_0 M_{23} \boldsymbol{I}_2 - \left(j\omega_0 L_3 + \frac{1}{j\omega_0 C_3} \right) \boldsymbol{I}_3 \end{cases} \tag{3}$$

The parameters of the transmitters I and II are designed to be identical, that is to say: $L_1 = L_2 = L$ and $L_{f2} = L_{f2} = L_f$. Substituting (1) and (2) into (3), the two transmitter currents and the output voltage can be expressed as follows:

$$\begin{cases} \boldsymbol{I}_1 = \frac{\boldsymbol{U}_1}{j\omega_0 L_f} = \frac{2\sqrt{2} U_{bus} e^{j0^\circ}}{j\pi\omega_0 L_f}, \boldsymbol{I}_2 = \frac{\boldsymbol{U}_2}{j\omega_0 L_f} = \frac{2\sqrt{2} U_{bus} e^{j\theta}}{j\pi\omega_0 L_f} \\ \boldsymbol{U}_3 = \frac{2\sqrt{2} U_{bus}}{\pi L_f} \left(M_{13} e^{j0^\circ} + M_{23} e^{j\theta} \right) \end{cases} \tag{4}$$

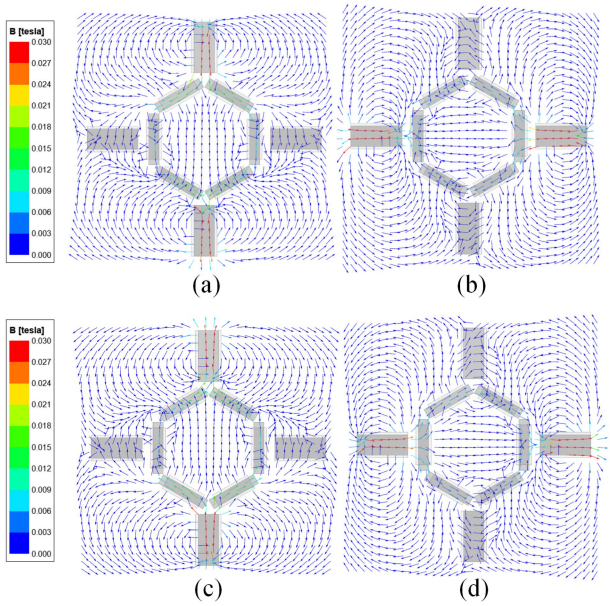

Fig. 4. Magnetic flux density vector in *YZ* plane during one switching period. (a) $t = 0$. (b) $t = T/4$. (c) $t = T/2$. (d) $t = 3T/4$.

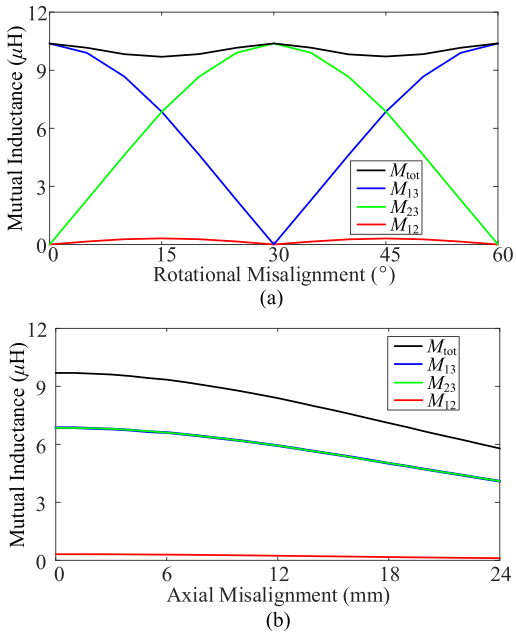

Fig. 5. Mutual Inductances of the proposed magnetic coupler. (a) Against the rotational misalignment. (b) Against the axial misalignment.

It can be seen that the total mutual inductance of the proposed WPT system can be expressed as follows:

$$M_{\text{tot}} = \left|M_{13}e^{j0^\circ} + M_{23}e^{j\theta}\right| = \sqrt{M_{13}^2 + M_{23}^2 + 2M_{13}M_{23}\cos\theta} \tag{5}$$

Then the output power can be obtained as

$$P_{\text{out}} = \frac{|\boldsymbol{U}_3|^2}{R_{\text{E}}} = \frac{U_{\text{bus}}^2}{L_{\text{f}}^2 R_{\text{L}}}\left(M_{13}^2 + M_{23}^2 + 2M_{13}M_{23}\cos\theta\right) \tag{6}$$

It can be seen that the output power is directly proportional to the square of M_{tot} when the other parameters keep constant. Therefore, the fluctuation of the output power will be enlarged by the fluctuation of M_{tot} during the rotational misalignment. To obtain the rotating magnetic field in all directions of YOZ plane, θ should be set to 90° [17]. Then M_{tot} can be simplified as

$$M_{\text{tot}} = \sqrt{M_{13}^2 + M_{23}^2} \tag{7}$$

The finite element analysis (FEA) method is utilized to analyze the characteristics of the proposed magnetic coupler. And the phase difference between the currents of the two transmitters is set to 90° in the simulation. Fig. 4 shows the magnetic flux density vector in the YZ plane during one switching period T. The case under $t = T$ is the same as that under $t = 0$, so it is not displayed in this figure. It can be seen that the magnetic field rotates in one period. Therefore, the receiver can obtain power from the rotating magnetic field when the rotational misalignment occurs.

Fig. 5 shows the mutual inductances of the transmitters and the receiver varying with the rotational and axial misalignments. It can be seen from Fig. 5(a) that the mutual inductance of the two transmitters M_{12} is close to zero due to their perpendicular magnetic fields. Moreover, M_{13} and M_{23} compensate each other. Thus, the total mutual inductance M_{tot} can remain relatively stable during the rotational misalignment. While M_{tot} has a 6.6% decrease under 15° of rotational misalignment compared to that under 0° case. Then the output power will have a 12.8% decrease based on (5). It can be seen from Fig. 5(b) that M_{13}, M_{23}, and M_{tot} decrease with the increasing axial misalignment. M_{tot} has a 6.5% decent when the axial misalignment is 8 mm, which is a third of the coil thickness, resulting in a 12.6% decrease in output power.

In order to have more stable output power with the minimal control variable, the phase difference between the two inverters θ can be regulated. The change rate of the output power can be defined as follows:

$$\delta = \frac{|P_{\text{out\_}\theta} - P_{\text{out\_0}^\circ}|}{P_{\text{out\_0}^\circ}} \times 100\% \le 5\% \tag{8}$$

where $P_{\text{out\_0}^\circ}$ is the output power when the rotational misalignment is 0° and the axial misalignment is 0 mm. Fig. 6 shows the output power fluctuation δ versus θ under the rotational and axial misalignments. It can be seen from Fig. 6(a) that when θ is adjusted in the range of 81°–99°, the output power fluctuation can be adjusted to be below 5%, which means the output power remains more stable.

The initial reference value of the phase angle difference θ is set to 90°. When there are rotational misalignments between the receiver and the two transmitters, the output power fluctuation will increase, as shown at point O in Fig. 6(a). 10° and 40° are taken as examples for detailed illustration. First, θ is controlled to decrease by two inverters. After sampling the output power, the controller calculates δ to judge the stepping direction through comparing it with that of the previous time. If δ is decreasing, such as the curve OP, keep the stepping direction constant until δ is less than δ_{ref}. On the contrary, if δ is increasing, such as the

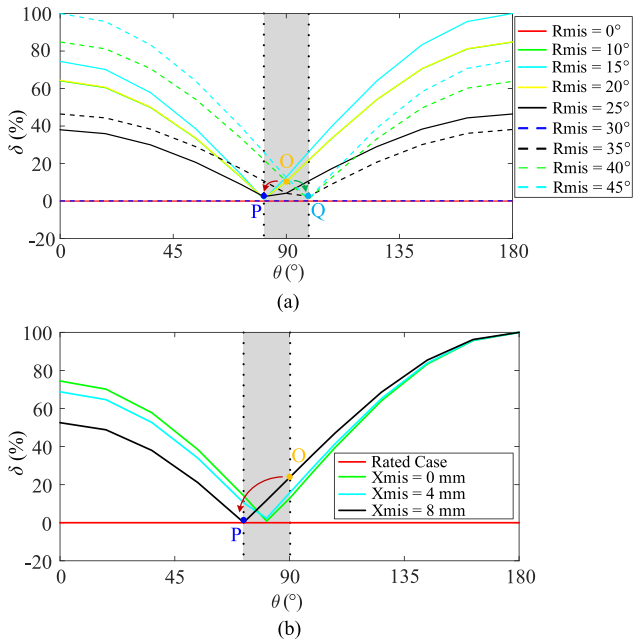

Fig. 6. Output power fluctuation versus θ. (a) Under the rotational misalignment. (b) Under the axial misalignment.

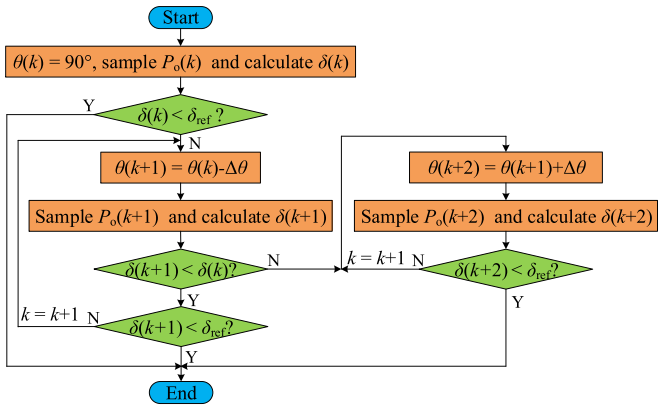

Fig. 7. Proposed control flow chart.

curve OQ, then reverse the stepping direction until δ is less than δ_{ref}. The proposed control flow chart is presented in Fig. 7.

As for the axial misalignment, the rated output power case is under the case that the rotational misalignment is 0° and the axial misalignment is 0 mm. It can be seen from Fig. 6(b) that the output power fluctuation is nearly the same as that of the half of the rotational misalignment. Then the curve OP can be used and keep the stepping direction constant until δ is less than δ_{ref}. Therefore, the proposed control method can be adapted to solve the axial misalignment issue.

IV. Experimental Verification

An experimental prototype based on the proposed magnetic coupler for the free-rotation WPT system is established, which is shown in Fig. 8. In the simulation and experiment, the rotational range is from 0° to 60° because the rotational period is 60°. The

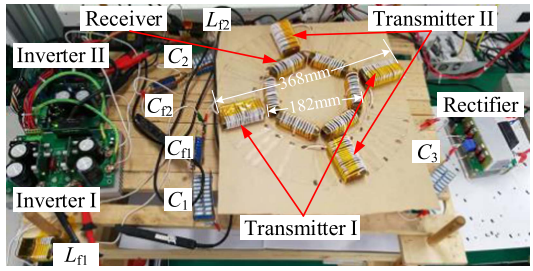

Fig. 8. Experimental prototype.

TABLE I
System Parameters

U_{bus}	L_1	L_2	L_3	L_{f1}	L_{f2}
110V	66.5 μH	66.6 μH	62.9 μH	8.9 μH	8.9 μH
M_{13}	M_{23}	M_{tot}	C_{f1}	C_{f2}	C_1
0.5 μH	10.1 μH	10.1 μH	71.3 nF	71.3 nF	10.5 nF
C_2	C_3	f_0	R_{L}	Single transmitter coil block dimension	
10.5 nF	10.2 nF	200 kHz	25 Ω	80mm×40mm×24mm	
Ferrite dimension in transmitter side		Single receiver coil block dimension		Ferrite dimension in receiver side	
80 × 32 × 16 mm		63 × 24 × 24 mm		80 × 16 × 16 mm	

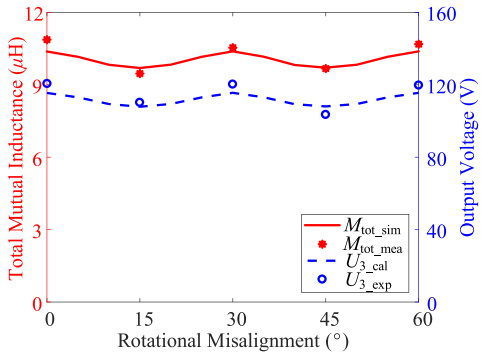

Fig. 9. Simulated and measured total mutual inductances and the output voltage versus the rotational misalignment.

adjacent receiver coils are wound reversely based on the design in Section II. Two full-bridge inverters are used to convert the power used to excite the two transmitter coils. Table I shows the system parameters.

The total mutual inductances and the output voltage of the proposed WPT system versus rotational misalignments are shown in Fig. 9. It can be seen that the total mutual inductance remains relatively stable against the rotational misalignment and the measured results are consistent with the simulated ones. Moreover, the output voltage can keep stable when the total mutual inductance remains constant based on the derivation of (4) in Section III, which verifies the theoretical analysis.

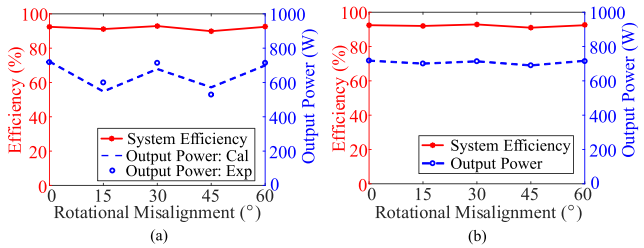

Fig. 10. DC–DC efficiency and output power versus the rotational misalignment. (a) Based on only magnetic coupler design. (b) Based on the composite method of magnetic coupler design and adjusting θ.

The dc–dc efficiency and output power versus the rotational misalignment is shown in Fig. 10(a). It can be seen that the system efficiency can remain relatively stable during the rotational misalignment. While there is a relatively large change in the output power. Based on the analysis in Section III, the output power is directly proportional to the square of the total mutual inductance when the other parameters are kept constant. Therefore, the fluctuation of the output power will be enlarged by the fluctuation of the total mutual inductance during the rotational misalignment.

In order to have more stable output power, the phase difference between the two inverters θ is regulated. Fig. 10(b) shows dc–dc efficiency and output power versus the rotational misalignment when adjusting θ, which indicates that more stable efficiency and output power are achieved. The output power fluctuation is below 5%.

V. Conclusion

In this letter, a free-rotation WPT system with segmented solenoid coils for AUVs is proposed to improve the rotational and axial misalignment tolerance. The magnetic coupler has two decoupled transmitters and one receiver with reversely wound adjacent receiver coils. The mutual inductances between the receiver and the two transmitters can compensate each other. Moreover, cooperated with the phase control between the two transmitters, the system can achieve stable output power under rotational and axial misalignment. A free-rotation WPT prototype was set up and the experimental results showed that the output power can reach 700 W and the output power fluctuation is below 5% based on the composite anti-misalignment method. Above all, it can only improve the misalignment tolerance to some extent via one anti-misalignment method. In order to further improve the misalignment tolerance in one direction or multidirection, the composite anti-misalignment method is necessary in the practical application.

References

[1] S. Li, S. Lu, and C. C. Mi, "Revolution of electric vehicle charging technologies accelerated by wide bandgap devices," *Proc. IEEE*, vol. 109, no. 6, pp. 985–1003, Jun. 2021.

[2] Y. Jiang, L. Wang, J. Fang, C. Zhao, K. Wang, and Y. Wang, "A joint control with variable ZVS angles for dynamic efficiency optimization in wireless power transfer system," *IEEE Trans. Power Electron.*, vol. 35, no. 10, pp. 11064–11081, Oct. 2020.

[3] Y. Zhang et al., "Integration of onboard charger and wireless charging system for electric vehicles with shared coupler, compensation, and rectifier," *IEEE Trans. Ind. Electron.*, 2022, doi: 10.1109/TIE.2022.3204857.

[4] J. Deng, Y. Zhang, S. Wang, Z. Wang, and Y. Yang, "The design and coupler optimization of a single-transmitter coupled multireceiver inductive power transfer system for maglev trains," *IEEE Trans. Transp. Electrific.*, vol. 7, no. 4, pp. 3173–3184, Dec. 2021.

[5] C. Yang, T. Wang, and Y. Chen, "Design and analysis of an omnidirectional and positioning tolerant AUV charging platform," *IET Power Electron.*, vol. 12, no. 8, pp. 2108–2117, Jul. 2019.

[6] Z. Yan, K. Zhang, L. Qiao, Y. Hu, and B. Song, "A multiload wireless power transfer system with concentrated magnetic field for AUV cluster system," *IEEE Trans. Ind. Appl.*, vol. 58, no. 1, pp. 1307–1314, Jan./Feb. 2022.

[7] J. Shi, D. Li, and C. Yang, "Design and analysis of an underwater inductive coupling power transfer system for autonomous underwater vehicle docking applications," *J Zhejiang Univ-Sci C*, vol. 15, no. 1, pp. 51–62, 2014.

[8] Y. Zeng et al., "Misalignment insensitive wireless power transfer system using a hybrid transmitter for autonomous underwater vehicles," *IEEE Trans. Ind. Appl.*, vol. 58, no. 1, pp. 1298–1306, Jan./Feb. 2022.

[9] C. Cai, S. Wu, Z. Zhang, L. Jiang, and S. Yang, "Development of a fit-to-surface and lightweight magnetic coupler for autonomous underwater vehicle wireless charging systems," *IEEE Trans. Power Electron.*, vol. 36, no. 9, pp. 9927–9940, Sep. 2021.

[10] T. Kan, Y. Zhang, Z. Yan, P. P. Mercier, and C. C. Mi, "A rotation-resilient wireless charging system for lightweight autonomous underwater vehicles," *IEEE Trans. Veh. Technol.*, vol. 67, no. 8, pp. 6935–6942, Aug. 2018.

[11] Z. Yan, B. Song, Y. Zhang, K. Zhang, Z. Mao, and Y. Hu, "A rotation-free wireless power transfer system with stable output power and efficiency for autonomous underwater vehicles," *IEEE Trans. Power Electron.*, vol. 34, no. 5, pp. 4005–4008, May. 2019.

[12] L. Zhao, D. J. Thrimawithana, and U. K. Madawala, "Hybrid bidirectional wireless EV charging system tolerant to pad misalignment," *IEEE Trans. Ind. Electron.*, vol. 64, no. 9, pp. 7079–7086, Sep. 2017.

[13] Y. Chen, S. He, B. Yang, S. Chen, Z. He, and R. Mai, "Reconfigurable rectifier-based detuned series-series compensated IPT system for anti-misalignment and efficiency improvement," *IEEE Trans. Power Electron.*, vol. 38, no. 2, pp. 2720–2729, Feb. 2023.

[14] T. Orekan, P. Zhang, and C. Shih, "Analysis, design, and maximum power-efficiency tracking for undersea wireless power transfer," *IEEE J. Emerg. Sel. Topics Power Electron.*, vol. 6, no. 2, pp. 843–854, Jun. 2018.

[15] K. Sasaki and T. Imura, "Combination of sensorless energized section switching system and double-LCC for DWPT," in *Proc. IEEE PELS Workshop Emerg. Technol., Wireless Power Transfer*, Seoul, Korea, 2020, pp. 62–67.

[16] H. R. Cha, K. H. Park, Y. J. Choi, and R. Y. Kim, "Double-sided LCC compensation topology with semi-bridgeless rectifier for wireless power transfer system," in *Proc. 10th Int. Conf. Power Electron. ECCE Asia*, Busan, Korea, 2019, pp. 1–6.

[17] H. Han, Z. Mao, Q. Zhu, M. Su, and A. P. Hu, "A 3D wireless charging cylinder with stable rotating magnetic field for multi-load application," *IEEE Access*, vol. 7, pp. 35981–35997, 2019.